

Nuclear-reaction analysis of H at the Pb/Si(111) interface: Monolayer depth distinction and interface structure

K. Fukutani,* M. Wilde, and M. Matsumoto

Institute of Industrial Science, The University of Tokyo, Komaba, Meguro-ku, Tokyo 153-8505, Japan

(Received 25 June 2001; published 29 November 2001)

Hydrogen atoms buried at the interface between Pb layers and the Si(111) surface were investigated by resonant nuclear reaction analysis (NRA) using $^1\text{H}(^{15}\text{N}, \alpha\gamma)^{12}\text{C}$ in grazing incidence geometry. Pb atoms were deposited on the H-terminated Si(111) surface at 110 K, and the H depth was clearly distinguished with a depth scale of one monolayer. The NRA spectrum revealed a monotonous shift to higher energy with increasing Pb coverage indicating H remains at the interface between Pb and the Si substrate. The dependence of the spectral shift on the Pb coverage was found to have an offset corresponding to a depth of about 0.1 nm. This offset suggests a model for the Pb/H/Si(111) interface structure implying that the initial Pb layer resides in the preadsorbed H layer.

DOI: 10.1103/PhysRevB.64.245411

PACS number(s): 68.35.Ct, 79.20.Rf, 68.55.-a

I. INTRODUCTION

Hydrogen interacting with solid surfaces and interfaces is of great importance and interest not only in fundamental physics and chemistry,^{1,2} but also in a variety of technological applications. Due to the light mass and small atomic size, H atoms tend to be absorbed by materials as demonstrated by hydrogen storage materials and are responsible for undesirable phenomena such as hydrogen embrittlement. In case of semiconductor technology, hydrogen at interfaces is practically interesting and important because of its influence on the Schottky-barrier height^{3,4} and its ability to reduce the density of the interface states by saturating dangling bonds. In the epitaxial growth of metals and semiconductors,⁵⁻⁷ hydrogen atoms sometimes modify the growth mode acting as a surfactant.

Despite the importance of H in a variety of surface and interface phenomena, H is visible to only a limited number of techniques, because of the small scattering factor due to its light mass and the small number of electrons available for electron spectroscopy. For the investigation of H at surfaces, subsurfaces, and interfaces therefore, a depth-resolved technique is strongly required. Resonant nuclear reaction analysis (NRA) (Refs. 8,9) and elastic recoil detection (ERD) (Refs. 5,10) enable depth-resolved measurements. In the previous publications, we investigated the formation of metal/H/Si(111) interfaces by NRA using the $^1\text{H}(^{15}\text{N}, \alpha\gamma)^{12}\text{C}$ reaction.^{11,12} In these studies, it was found that an interface layer of H atoms is formed between a Pb overlayer and a Si substrate and the deposited Pb atoms form a uniform layer at 110 K. Compared with the Pb/Si(111) interface,^{13,14} a H-induced dipole layer was suggested to be present at the interface modifying the Schottky-barrier height,⁴ but the real interface structure is not known yet. The depth resolution (the spectral width divided by the stopping power) at normal ion beam incidence on the sample turned out to be ~ 5 nm,^{11,12} i.e., twenty monolayers (ML) of Pb, which is mainly determined by the zero-point vibration of H against the surface and the straggling of the ^{15}N ions in the Pb overlayers. For further detailed studies of subsurface occupation

and early stages of interface formation, improvement of the depth resolution is highly required. Therefore the first aim of the present paper is to improve the depth resolution by changing the incidence angle of the ion beam: the effective thickness experienced by the ^{15}N ion traveling through an adlayer is increased in a tilted geometry. Here we report NRA measurements of H buried at the interface between a Si(111) substrate and thin Pb overlayers (0.8–5 ML) taken in grazing beam incidence geometry, and achieved atomic-layer depth distinction of hydrogen. The dependence of the H-depth profile on the Pb coverage allows us to discuss the initial stage of the Pb/H/Si interface formation and to derive a model of the interface structure.

II. EXPERIMENT

The experimental setup is described elsewhere.¹² Briefly, the sample preparation and NRA measurements were performed in a UHV chamber (base pressure: $< 1 \times 10^{-8}$ Pa) at the 2C beam line of the tandem-type Van de Graaff accelerator at the Research Center for Nuclear Science and Technology of the University of Tokyo. The $^{15}\text{N}^{2+}$ ion beam at an energy around 6.385 MeV produced by this accelerator was introduced into the UHV chamber for the NRA measurement. The nuclear reaction we used is $^1\text{H}(^{15}\text{N}, \alpha\gamma)^{12}\text{C}$, which is resonanced at a $^{15}\text{N}^{2+}$ energy of 6.385 MeV with a resonance width of 1.8 keV.^{15,16} Detection of γ rays with an energy of 4.43 MeV by a $\text{Bi}_4\text{Ge}_4\text{O}_{12}$ scintillator placed at a distance of 40 mm behind the sample enables us to measure the H concentration. Furthermore, variation of the ion energy gives us the depth information of H atoms. The energy width of the incident ion beam was 3 keV, which was achieved by monochromatization with the energy analyzer (dispersion: 2560 mm) at a slit width of 1.2 mm and with the help of a slit feedback system. The typical beam current and beam size at the sample were 30 nA and 2 mm in diameter, respectively. The NRA measurements in the present work were conducted at an ion incidence angle of 80° with respect to the surface normal. Special care was taken concerning the sample position against the ion beam, because striking of the beam at any surfaces other than the sample increases the

background signal. The γ -ray yield was normalized by the sample current integrated over the acquisition time of 100 s per data point. The spectra shown in the present paper, unless otherwise stated, are the average of two independent spectra to reduce experimental uncertainty. Since the ion current density at the sample surface is lower than that at a normal incidence by a factor of $\cos 80^\circ$, the decay of the γ -ray yield due to ion-induced desorption can be neglected.¹²

The sample used in the present study is Si(111)1 \times 1-H, which was prepared by dosing atomic H at a sample temperature of 650 K until the H coverage was saturated.¹⁷ Before dosing atomic H, the Si(111) sample ($8 \times 50 \times 0.5$ mm³) was cleaned by resistively flashing in UHV to 1370 K until LEED reveals a clear 7 \times 7 pattern. Atomic hydrogen was produced by a tungsten filament heated at 1900 K, which is mounted in a molybdenum tube and placed at a distance of about 100 mm from the sample. After H dosage, the sample exhibited a clear 1 \times 1 LEED pattern indicating the formation of a H-terminated Si(111) surface. Below 400 K, the sample temperature was measured by a Chromel-Alumel thermocouple attached to the Ta electrode supporting the Si sample, while temperatures higher than 700 K were measured with an optical pyrometer. The evaporation of Pb was performed using a tungsten filament and the evaporation rate was measured by a quartz oscillator placed below the sample. The typical evaporation rate was 0.01 nm/s. The metal-deposited surfaces were characterized by LEED and Auger electron spectroscopy (AES). The sample temperature during the metal evaporation was kept at 110 K. During the NRA measurements, the beam irradiation might have caused a local temperature rise of the surface up to about 150 K even though the sample was kept cooled by liquid nitrogen.

III. RESULTS AND DISCUSSION

Figure 1 shows the γ -ray intensity as a function of the incident ¹⁵N beam energy (NRA spectrum) taken from Si(111)1 \times 1-H after Pb deposition of 0.20 nm (0.84 ML). The profile reveals a peak near the resonance energy of 6.385 MeV. The solid curve is a fit to a Gaussian function of the form of $A \exp[-\{(E-E_R)-E_0\}^2/\sigma^2]$, where E is the ion energy, E_R is the resonance energy of 6.385 MeV, and A , E_0 , and σ are fit parameters. Also shown in Fig. 1 by a dashed curve is a fit curve of the spectrum taken for the pure Si(111)1 \times 1-H substrate before Pb deposition. [The data points are shown in Fig. 2(a).] The results show that the peak of the NRA spectrum after Pb deposition is shifted to higher energy compared to the bare Si(111)-H substrate. The peak shift deduced from the fits amounts to 0.66 ± 0.11 keV. The spectral width (σ) obtained from the fit is 6.43 ± 0.11 keV, which is slightly broader than the width of 5.90 keV for Si(111)1 \times 1-H. Assuming that the H coverage on the clean Si(111)1 \times 1-H surface is 1 monolayer (ML), the H coverage after Pb deposition was estimated to be 1.01 ± 0.07 ML by comparing the integrated areas of the spectra.

The NRA spectra taken after Pb deposition of 0.37 and 1.11 nm (1.56 and 4.68 ML, respectively) on Si(111)1 \times 1-H are shown in Fig. 2(a). Note that LEED exhibited a clear 1

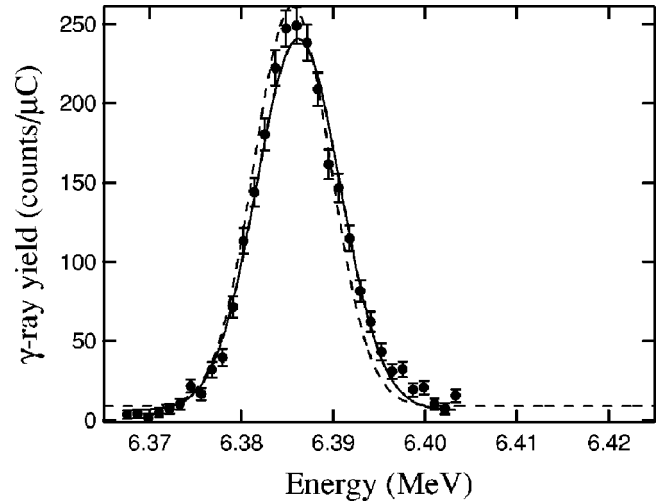


FIG. 1. Intensity profile of the γ ray from the $^1\text{H}(^{15}\text{N}, \alpha\gamma)^{12}\text{C}$ nuclear reaction as a function of the incident ^{15}N beam energy taken for the sample of Pb deposition of 0.20 nm on the Si(111)1 \times 1-H at a sample temperature of 110 K. Solid curve is a fit to a Gaussian form and the dashed curve denotes a fit to the spectrum before the Pb deposition.

\times 1 pattern without noticeable changes after the Pb deposition. In Fig. 2(a), the peak shifts are more pronounced compared to Fig. 1. After 1.11 nm of Pb deposition, the spectrum exhibits a peak shift as much as 10 keV together with a substantial decrease of the peak height and an increase of the spectral width. Both spectra are fitted to a Gaussian form which are displayed by the solid curves in the figure and the fit parameters obtained are listed in Table I. The H concentrations estimated from the integrated areas of the spectra are 1.16 ± 0.08 and 0.90 ± 0.08 ML for Pb coverages of 0.37 and 1.11 nm, respectively. Therefore, the initial H is concluded to be preserved after Pb deposition, which is in agreement with our previous results.¹² Since the peak of the NRA spectrum shifts to higher energy with increasing Pb coverage, the H atom preadsorbed on Si(111) is, furthermore, considered to remain at the interface between the Si(111) substrate and the Pb overlayer, which is also consistent with the previous studies.^{4,12} These data therefore emphasize the fact that the NRA technique in grazing incidence geometry has the capability to distinguish changes of the hydrogen depth due to metal overlayers within the submonolayer regime.

By using the E_0 value representing the peak shift with respect to the resonance energy, we can calculate the mean depth of H. With the stopping power of Pb for ^{15}N at 6.385 MeV, 2.32 keV/nm,^{18,19} the H depths for the three samples are calculated to be 0.28, 1.09, and 4.58 nm, respectively. Assuming that the Pb atoms form a uniform layer, the thickness of the Pb overlayer is estimated to be 0.049, 0.189, and 0.795 nm taking account of the incidence angle (θ) of 80° . Figure 2(b) shows the relation between the thickness estimated from the NRA spectra and the deposited amount of Pb measured by the quartz oscillator. A fit to a linear relation is displayed by the solid line in the figure, which does not cross the origin indicating that the thickness estimated by NRA has an offset of -0.118 ± 0.013 nm. This corresponds to

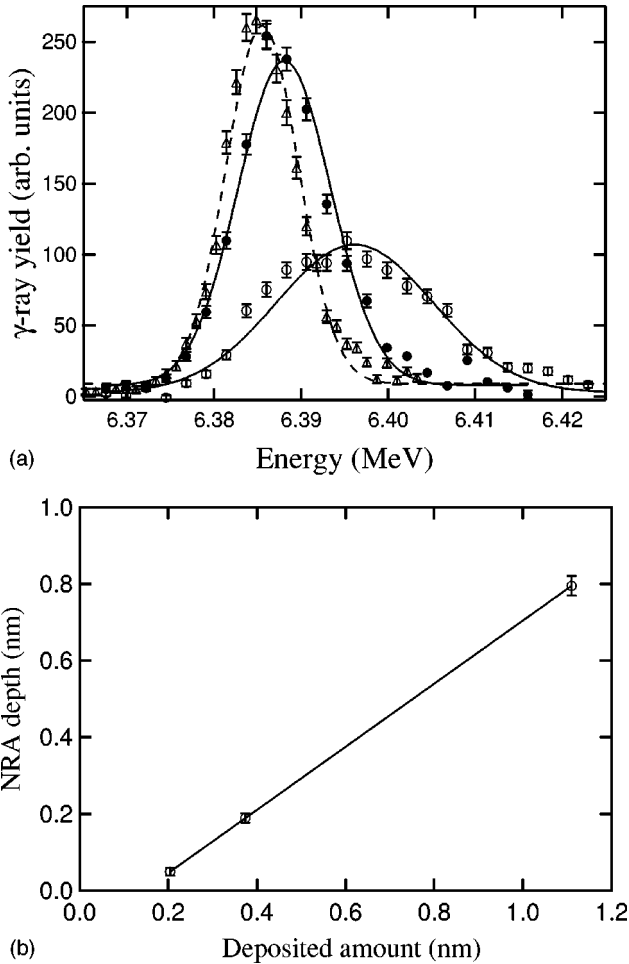


FIG. 2. (a) Intensity profile of the γ ray from the $^1\text{H}(^{15}\text{N}, \alpha\gamma)^{12}\text{C}$ nuclear reaction as a function of the incident ^{15}N beam energy taken for the $\text{Si}(111)1\times 1\text{-H}$ surface before Pb deposition (triangle) and after Pb deposition of 0.37 nm (filled circles) and 1.11 nm (open circles) at 110 K. Solid and dashed curves are fits of the spectra to a Gaussian form. (b) Relation between the Pb thickness estimated from the shift of the NRA spectra and the deposited amount measured by the quartz oscillator. Solid line is a fit to a linear relation.

$\sim 50\%$ of a monolayer and is not experimental error. It appears as if the first 0.5 ML of the deposited Pb did not stick to the surface. We consider, however, that this offset reflects the structure of the Pb-Si interface. The gradient of the fit line in Fig. 2(b) is smaller than unity by 18%, which is easily understood in terms of slight underestimations of the ion incidence angle and/or quartz oscillator position. However, the relative value measured by the quartz oscillator is quite

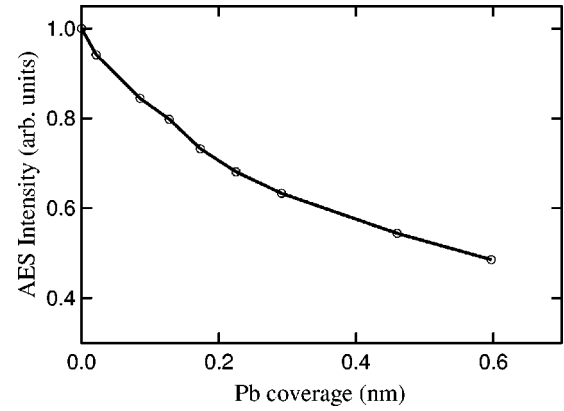


FIG. 3. Evolution of the Auger intensity at about 90 eV corresponding to superposition of Si LVV and Pb NOO as a function of the deposited amount of Pb measured by the quartz oscillator on $\text{Si}(111)1\times 1\text{-H}$ at 110 K.

accurate within a few % of a monolayer. We note that such an underestimation of the angle or distance influences only the gradient of the relation in Fig. 2(b) but would never cause an offset.

We can conceive three possible reasons for the offset in Fig. 2(b): change of the sticking probability, electronic modification and geometric structure. If the sticking probability of Pb atoms for the initial first layer is substantially lower than that of the second layer, the actual thickness observed by NRA becomes smaller than the deposited amount measured by the quartz oscillator at the initial stage of the growth. However, this possibility is excluded by AES data taken during Pb deposition. Figure 3 shows the evolution of the Auger intensity at about 90 eV corresponding to superposition of Si LVV and Pb NOO as a function of the deposited amount of Pb on $\text{Si}(111)1\times 1\text{-H}$. Although the two Auger lines are superimposed, Si LVV is dominant over Pb NOO in this coverage region. As seen in Fig. 3, the Auger intensity decreases monotonously from the beginning without showing any abrupt changes of the sticking probability.

If the electron density in the first Pb layer were substantially depleted due to a possible charge transfer to the substrate, the stopping power of this layer for the ^{15}N ion would be reduced compared with the value we used representing bulk Pb. Considering, however, the fact that the Si surface is well passivated by H atoms and rather inactive to other gas molecules, a large charge transfer between the substrate and Pb ad-atoms does not appear probable. Hence, we exclude possible electronic effects as the origin of the offset. As for the possibility of geometric effects, the offset might indicate that the first 0.1 nm of Pb could be located within or beneath

TABLE I. Parameters obtained from the fits of NRA spectra at different Pb coverages to a Gaussian form of $A \exp[-\{(E - E_R) - E_0\}^2/\sigma^2]$.

Pb coverage (nm)	0	0.20	0.37	1.11
E_0 (keV)	0	0.66 ± 0.11	2.53 ± 0.11	10.62 ± 0.21
σ (keV)	5.90 ± 0.10	6.43 ± 0.11	7.54 ± 0.13	12.78 ± 0.30
A	253 ± 4.8	234 ± 4.8	229 ± 4.5	104 ± 2.5

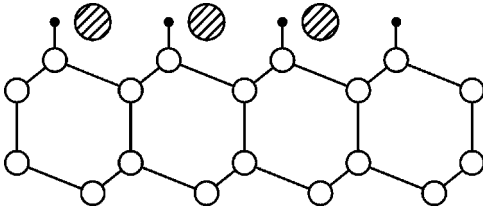


FIG. 4. Side view of the schematic model for the initial adsorption of Pb on Si(111)1 \times 1-H at 110 K. Filled, open, and shaded circles denote H, Si, and Pb atoms, respectively.

the H layer. Since the experiment was performed at 110 K, the Pb-Si interdiffusion and Si-H bond restructuring may be neglected, which is indirectly supported by the fact that H remains at the Pb-Si interface even at 300 K. As a naive model, we propose that in the initial stage of the interface formation Pb atoms occupy the threefold hollow sites of the H-terminated Si(111)1 \times 1 surface residing in the H layer to a certain extent as schematically shown in Fig. 4. These Pb atoms only partially shade the H atoms from the ion beam causing an offset in the Pb overlayer thickness monitored by NRA. It should be noted that the atomic radius of Pb is 0.146 nm, which can be reconciled with the nearest-neighbor distance of 0.384 nm between H atoms on Si(111). The Schottky barrier height for the Pb contact formed on Si(111)1 \times 1-H is reported to be higher than that formed on the bare Si(111) surface by 0.08 eV and a H-induced dipole layer has been suggested as a possible explanation.^{4,20} The present data may offer a clue to the interface structure of Pb/H/Si(111), and with electronic structure calculations the mechanism of the change of the Schottky barrier height would be clarified.

The Pb atoms deposited at 110 K were found to grow in a uniform layer at a coverage of 20 ML.¹² At room temperature, on the other hand, it is reported that Pb atoms undergo a three-dimensional (3D) island growth.^{12,21,22} On Si(111)7 \times 7, it is reported that Pb forms multistep height islands.²³ One might consider that the deposited Pb atoms form small islands in the early stage of the growth at 110 K and that such 3D islands instead of a uniform layer affect the effective energy loss of the incident ion leading to underestimation of the thickness by NRA. Nevertheless, this effect can be neglected in the first approximation as discussed below. For discussing such a possible effect of Pb islands, we model the overlayer morphology instead of a uniform layer as regularly arranged one-dimensional islands with H atoms at the uncovered substrate surface and at the interface between the substrate and the Pb overlayer as shown in Fig. 5(b), where D , t , T , and d ($=Dt/T$) are island height, island length, distance between the island centers, and average coverage of the overlayer. At a given coverage (d), the NRA spectrum changes depending on the relation of D , T , and θ (incidence angle of the ion). As laid out in detail in the Appendix, the NRA spectrum, in the case of $D \tan \theta < T$, i.e., the fraction of the uncovered Si-H surface shaded by the Pb island is smaller than the distance between the Pb islands, reveals two separate peaks corresponding to depths of 0 and $D/\cos \theta$ (or $t/\sin \theta$), which is well demonstrated in the normal incidence condition¹² and in experiments of In deposition on

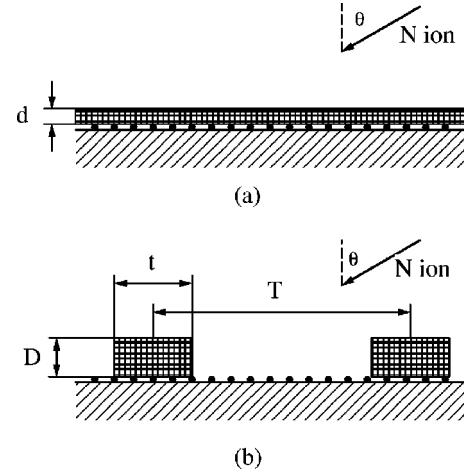


FIG. 5. Schematic figures of (a) layer growth and (b) three-dimensional island growth. D , t , and T are island height, island length, distance between islands.

Si(111)-H.²⁴ In the case of $D \tan \theta \geq T$, on the other hand, the spectrum is expected to exhibit a single peak at an energy corresponding to a depth of $d/\cos \theta$ with a broadening of the spectral width. It is worth noting that the apparent spectral depth averaging over all signal contributions from the uncovered Si-H surface and the interface below the Pb islands is given by $d/\cos \theta$ in both cases. The experimental results shown in Figs. 1 and 2 exhibit a single peak excluding the situation of $D \tan \theta < T$. Consequently, even if the Pb atoms deposited on the Si(111)-H surface did not grow as a uniform layer forming three-dimensional islands in the early stage of the growth, the average thickness apparent in NRA spectra would have to be described as $d/\cos \theta$, which is the same result as observed for a uniform layer. Therefore, the offset observed in Fig. 2(b) can be ascribed to the interface structure reflecting the relative position between H and Pb, rather than being a result of the Pb overlayer morphology.

It is noticed that the spectral width becomes broader with increasing Pb coverage as shown in Table I. The width of the NRA spectrum is essentially determined by the following factors: the natural reaction width, instrumental width, zero-point vibration, H depth distribution, and energy straggling.⁸ Since the ion beam suffers from no straggling for H on the surface, the width of the spectrum before Pb deposition represents the former three factors. The spectral broadening, therefore, originates from the H depth distribution and/or energy straggling. According to Bohr's expression, the energy straggling (Ω) of high-energy ions in solids is proportional to the square root of the ion-transmitting thickness (t) as described by $\Omega = \sqrt{Qt}$ where Q is the straggling cross section.²⁵ Since the Q value for the ¹⁵N ion at ~ 6.4 MeV is not established yet,²⁵⁻²⁷ unfortunately, we tentatively follow the empirical formula obtained by Rud *et al.*,²⁵ where FWHM due to the energy straggling in the Pb layer is described as $5.7 \times \sqrt{t[\text{nm}]} [\text{keV}]$. The effective Pb thicknesses of the samples in Figs. 1 and 2 are 0.28, 1.09, and 4.58 nm, which are obtained from the shift of the NRA spectrum (E_0), and the corresponding energy straggling are calculated to be 3.0, 5.9, and 12.2 keV, respectively. Assuming that both en-

ergy straggling and the spectrum before deposition are described by a Gaussian form, convolution of these two terms leads to total widths of 10.3, 11.5, and 15.6 keV, which are smaller than the experimental values of 10.7, 12.6, and 21.3 keV, respectively. Since the difference becomes larger with increasing thickness, the discrepancy is not due to the change of the vibrational frequency of H buried at the interface. The difference can be ascribed to the H depth distribution due to morphological roughness of the Pb layer and/or an underestimation of the energy straggling. Assuming that the difference originates solely from the H depth distribution and the distribution is described by a Gaussian form, by deconvoluting the straggling width, the width (FWHM) of the H distribution is estimated to be 1.3, 2.3, and 6.3 nm. Considering the mean H depth of 0.28, 1.09, and 4.58 nm for the three samples, respectively, the depth distribution seems to be too large. This might indicate that the Q value for the straggling width needs to be modified.

IV. CONCLUSION

Pb deposition on the H-terminated Si(111) surface at 110 K in the monolayer regime was investigated by NRA using $^1\text{H}(^{15}\text{N}, \alpha\gamma)^{12}\text{C}$ in grazing incidence of 80° with respect to the surface normal. The NRA spectrum revealed a clear shift after Pb deposition of 0.20 nm implying that the H depth can be distinguished on a depth scale of one monolayer. The dependence of the spectral shift on the Pb coverage was found to have an offset corresponding to a depth of about 0.1 nm. This offset suggests that the initial Pb layer resides in the pre-adsorbed H layer as it forms the Pb/H/Si(111) interface. The width of the NRA spectrum was found to increase substantially with increasing Pb coverage, and the origin of this broadening was discussed in terms of energy straggling of the ^{15}N ion and the H depth distribution.

ACKNOWLEDGMENTS

The authors are grateful to H. Yamashita, K. Kobayashi, H. Matsuzaki, and C. Nakano for their experimental assistance for the accelerator operation. This work was supported

by a Grant-in-Aid for Scientific Research and COE Research from the Ministry of Education, Science, Sports and Culture of Japan.

APPENDIX

When the deposited atoms form a completely uniform layer with a thickness of d as shown in Fig. 5(a), the depth of H below the overlayer is observed to be $d/\cos\theta$ by NRA. If the atoms grow as 3D islands, on the other hand, the NRA spectrum is accordingly modified depending on the island size and density and the ion incidence angle. We model the overlayer structure as regularly arranged one-dimensional islands as shown in Fig. 5(b). With a fixed coverage of d ($=Dt/T$) and incidence angle of θ , the H depth distribution observed by the ion beam is classified into six cases depending on the relation of D , t , T , and θ .

(1) $D \tan\theta \ll t$. The ion sees H on the Si surface with a depth of 0 as well as H at the Pb-Si interface as a depth of $D/\cos\theta$. Therefore, the NRA spectrum reveals two peaks at energies corresponding to the two depths.

(2) $D \tan\theta < t$. In addition to the distinct peaks corresponding to the depths of (1), a continuous distribution is observed at depths between 0 and $D/\cos\theta$ because of the partial shading of H by the island edge.

(3) $t < D \tan\theta < T$. Similarly to (2), H is observed at depths of 0 and $t/\sin\theta$ with a small continuous distribution between 0 and $t/\sin\theta$.

(4) $mT = D \tan\theta$ where m is a natural number. The depth observed by NRA becomes $d/\cos\theta$ for both surface and interface H atoms revealing a corresponding single peak in the spectrum.

(5) $T < D \tan\theta$ except (4). The ion comes through $\sim n$ islands before reaching H atoms where n is the quotient of $D \tan\theta/T$. The H atom is hence observed to be distributed from a depth of $nt/\sin\theta$ to $(n+1)t/\sin\theta$ implying the distribution width of $t/\sin\theta$, and the average depth is calculated to be $d/\cos\theta$.

(6) $T \ll D \tan\theta$. The H depth is observed to be $d/\cos\theta$.

It should be noted that the depth averaged over all signals in each case becomes $d/\cos\theta$.

*Electronic address: fukutani@iis.u-tokyo.ac.jp

¹K. Christmann, Surf. Sci. Rep. **9**, 1 (1988).

²W. A. Dino, H. Kasai, and A. Okiji, Prog. Surf. Sci. **63**, 63 (2000).

³W. Mönch, Phys. Low-Dimens. Semicond. Struct. **4/5**, 1 (1994).

⁴T. U. Kampen and W. Mönch, Surf. Sci. **331-333**, 490 (1995).

⁵M. Copel and R. M. Tromp, Phys. Rev. Lett. **72**, 1236 (1994).

⁶K. Oura, V. G. Lifshits, A. A. Saranin, A. V. Zotov, and M. Katayama, Surf. Sci. Rep. **35**, 1 (1999), and references therein.

⁷A. Sakai and T. Tatsumi, Appl. Phys. Lett. **64**, 52 (1994).

⁸W. A. Lanford, Nucl. Instrum. Methods Phys. Res. B **66**, 65 (1992).

⁹G. Amsel and B. Maurel, Nucl. Instrum. Methods **218**, 183 (1983).

¹⁰K. Kimura, K. Nakajima, and H. Imura, Nucl. Instrum. Methods Phys. Res. B **140**, 397 (1998).

¹¹K. Fukutani, H. Iwai, H. Yamashita, Y. Murata, S. Hatori, and K. Kobayashi, Surf. Sci. **377-379**, 1010 (1997).

¹²K. Fukutani, H. Iwai, Y. Murata, and H. Yamashita, Phys. Rev. B **59**, 13 020 (1999).

¹³E. Ganz, I.-S. Hwang, F. Xiong, S. K. Theiss, and J. Golovchenko, Surf. Sci. **257**, 259 (1991).

¹⁴J. A. Carlisle, T. Miller, and T.-C. Chiang, Phys. Rev. B **45**, 3400 (1992).

¹⁵B. Maurel and G. Amsel, Nucl. Instrum. Methods **218**, 159 (1983).

¹⁶M. Zinke-Allmang, S. Kalbitzer, and M. Weiser, Z. Phys. A **320**, 697 (1985).

¹⁷F. Owman and P. Mårtensson, Surf. Sci. **303**, L367 (1994).

¹⁸*Handbook of Stopping Cross-Sections for Energetic Ions in All Elements* (Pergamon, New York, 1980).

- ¹⁹*Handbook of Modern Ion Beam Materials Analysis*, edited by J. R. Tesmer and M. Nastasi (Materials Research Society, Pittsburgh, 1995).
- ²⁰D. R. Heslinga, H. H. Weiering, D. P. van der Werf, T. M. Klapwijk, and T. Hibma, *Phys. Rev. Lett.* **64**, 1589 (1990).
- ²¹S. Odasso, L. Seehofer, and R. L. Johnson, *Appl. Surf. Sci.* **137**, 71 (1999).
- ²²J. C. Ziegler, G. Scherb, O. Bunk, A. Kazimirov, L. X. Cao, D. M. Kolb, R. L. Johnson, and J. Zegenhagen, *Surf. Sci.* **452**, 150 (2000).
- ²³K. Budde, E. Abram, V. Yeh, and M. C. Tringides, *Phys. Rev. B* **61**, 10 602 (2000).
- ²⁴M. Wilde, M. Matsumoto, and K. Fukutani (unpublished).
- ²⁵N. Rud, J. Bottiger, and P. S. Jensen, *Nucl. Instrum. Methods* **151**, 247 (1978).
- ²⁶M. A. Briere and J. P. Biersack, *Nucl. Instrum. Methods Phys. Res. B* **64**, 693 (1992).
- ²⁷P. Goppelt-Langer, S. Yamamoto, Y. Aoki, H. Takeshita, and H. Naramoto, *Nucl. Instrum. Methods Phys. Res. B* **118**, 7 (1996).